

The Effect of Brain Tumors on Local SAR Levels at 7T

Matthew C. Restivo¹, Cornelis A.T. van den Berg¹, Astrid L.H.M.W. van Lier¹, Daniël L. Polders¹, Alexander J.E. Raaijmaker¹, Peter R. Luijten¹, and Hans Hoogduin¹
¹Imaging Division, University Medical Center Utrecht, Utrecht, Netherlands

Introduction: RF energy absorption has the potential to result in significant localized tissue heating if not properly monitored. Current SAR monitoring practices involve using generic patient models to evaluate the RF energy absorption, quantified by the global and local Specific Absorption Rate (SAR) distribution. Already, research has shown that patient variability can have a significant impact on predicted SAR values¹. This study looks to answer questions related to predicting global and local SAR in patients whose anatomies differ greatly from the generic model. Specifically, we want to analyze the effect of brain tumors on local SAR levels at 7T. It is known from a previous study employing Electric Property Tomography (EPT) that tumor conductivity is typically higher than normal brain tissue². Given that SAR is related to conductivity with the relationship [SAR \propto $\sigma|E|$ ²], we might expect that patients with brain tumors will have significantly increased local SAR values at the tumor locations during RF excitation. In this study, we used EM simulation tools to estimate 10g averaged local SAR (SAR_{10g}) using realistic brain models and conductivity values from EPT scans of three tumor patients. We also looked at the effect of sweeping the tumor conductivity parameter to account for tumor variability.

Methods: The models used for our EM simulations were created using anatomical scans and conductivity values derived from the work of Van Lier et al². We first segmented 3T T1w contrast enhanced brain scans of the 3 patients to create dielectric models of their brains. To mitigate the challenges associated with segmenting the entire head, we chose to only segment each brain into five tissue types: grey matter, white matter, cerebral spinal fluid (CSF), contrast enhancing tumor, and non-contrast enhancing tumor. The three non-tumor tissue types were segmented using the automatic segmentation functionality provided by 3D Slicer³. This segmentation also served as the tumor-free control model. Next, we manually segmented tumor tissue using iSeg (Speag AG, Zurich, Switzerland). In the T1w images, we observed that the tumors are composed of two distinct regions, a region that is enhanced by contrast and a region that is not enhanced (Fig. 1A). It is important to make this distinction because Van Lier et al. observed that these regions have different average conductivity values when measured through EPT². Analysis of the three 7T EPT scans of these patient revealed an average conductivity for enhancing and non-enhancing regions of 0.88 S/m and 1.56 S/m respectively. Subsequently, the complete dielectric brain models were imported into the numerical EM solver (SEMCAD, Speag AG, Zurich, Switzerland) for simulation. To account for the fact that we only segmented the patient's brain, we combined our segmentation model with a generic head model so that our simulations would include EM effects caused by the skull, internal air cavities, and other head tissues. Ella, from the Virtual Family⁴, was used as the generic patient model. We combined the real patient brain model with the generic patient model by centering the brain in the skull of Ella and scaling Ella so that the head conformed to the shape of the real patient's brain. Fig. 1A and Fig. 1B show the anatomical scans for each patient compared with the geometry of the model used for simulation. We do not have measured values for the dielectric permittivity and densities of each tumor, so we assume those values are the same as that of nearby, similar tissue types. A complete list of SAR related tissue parameters is shown in table 1. We additionally analyzed the effect of assigning arbitrary average tumor conductivity over a range from 0.5 to 3.0 S/m.

FDTD simulations were performed using a realistic 298 MHz resonant birdcage coil operating in quadrature. The head of the model was placed in the center of the coil approximating a realistic positioning for a 7T brain scan. SAR_{10g} results were normalized so that the average whole head SAR was 3.2 W/kg in the healthy model.

Results: For each of the three patients, the SAR_{10g} distribution from the model containing a tumor was compared to the model without the tumor (Fig. 1C and Fig. 1D). In all tumor patients, local SAR was increased at the location of the tumor. The peak SAR_{10g} over the whole head, however, did not occur at the tumor site. Peak SAR_{10g} values occurred at the boundaries of the brain, typically near the skull where the E-fields are the strongest. Thus, the increase in SAR_{10g} in the location of the tumor did not exceed the tumor-free peak value in all 3 patient cases. Also, the whole head peak SAR_{10g} was mostly unaffected by the presence of the tumor (Fig. 2).

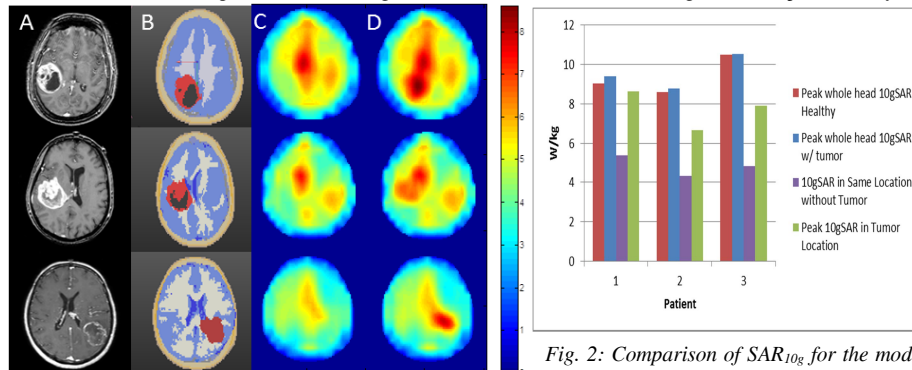


Fig. 1A-D: Simulated SAR_{10g} for patients 1-3. A: Anatomical T1w contrast enhanced patient scans B: Dielectric model with tumor present. C: SAR_{10g} (W/kg) without tumor. D: SAR_{10g} (W/kg) with tumor.

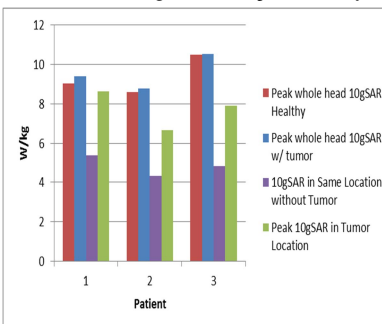


Fig. 2: Comparison of SAR_{10g} for the model with the tumor and without the tumor. Peak SAR_{10g} over the whole head does not change much; however, SAR at the site of the tumor increases significantly.

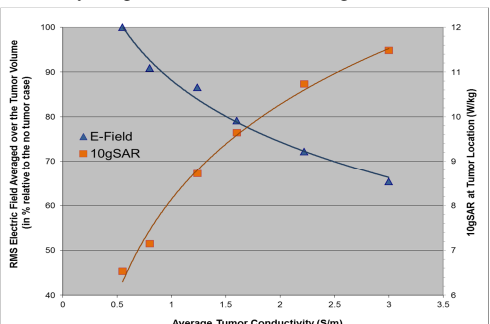


Fig. 3: Effect of changing conductivity on local E-field strength and local SAR in the tumor of patient 2. Lines show trend line fit with logarithmic regression. It is not until tumor conductivity reaches the level of CSF that local SAR becomes unsafe according to the accepted SAR_{10g} limit of 10 W/kg.

Discussion: The increased conductivity of brain tumors can lead to an increase in local SAR. However, our results show that the increase in SAR is not proportional to the increase in conductivity. While the conductivity of a tumor is approximately 2-3 times the conductivity of the surrounding tissue, the SAR_{10g} only increases by 30-60% (Fig. 2,3). This can be explained by the electric field shielding effect of good conductors. The strength of the electric field in the region of the tumor is inversely related to the tumor conductivity (Fig. 3). Additionally, we can show that increasing the conductivity of the tumor above realistic values still only results in a marginal SAR increase due to this shielding effect.

Conclusion: Our simulations show that the presence of a brain tumor in the studied patients, which leads to an area of the brain having higher than normal conductivity, only leads to moderate increase in tumor SAR values. Assuming that the tumor is contained within the brain, we expect that peak SAR_{10g} in the tumor is less than the predicted whole head peak local SAR value using a patient model without the tumor. However, caution has to be taken for tumors that are located in regions with strong electric fields such as near the skull.

References: (1) de Gref et al. MRM, 2013, 69:1476–1485. (2) Van Lier et al. ISMRM 2011 p. 4464. (3) 3D Slicer (<http://slicer.org>). (4) Christ et al. PMB 2010, 55:N23-N38. This study was part of the FP7 HiMR Project